On Silicon Group Elements Ejected by Supernovae Type Ia

What are the observational implications of the different combustion mechanisms for the different models?

Soma De, Frank Timmes,
E. Brown, A. Calder, D. Townsley,
D. Jack, D. Chamulak, W. Hawley, T. Athanassiadou

SCHOOL OF EARTH & SPACE EXPLORATION
ARIZONA STATE UNIVERSITY

SPIDER

MESA

JINA

If the composition of the white dwarf has an observable effect on the ^{56}Ni production and thus the SNIa light curve, it could have an effect on other elements as well.

We present a new tool which connects the electron fraction Y_e in the silicon-rich regions of individual SNIa to the observed Si, S, Ca, and Fe abundances. This may also be a useful tool for distinguishing one & two white dwarf progenitor scenarios.

The method follows from ^{28}Si, ^{32}S, ^{40}Ca and ^{54}Fe being
(a) produced in QNSE and that
(b) these abundance levels do not change during the subsequent freezeout as the SNIa expands.

Thus, the observed photospheric abundances of these elements are related to each other through thermodynamics, are independent of SNIa model parameters, and recorded in the observed spectra.

From the observed abundances, our method applies the QNSE relations (in reverse!) to determine the abundances and hence a measure of Y_e in the silicon group regions.

The method begins with mass & charge conservation, and the constraints for a two-cluster QNSE:

$$Y_n + Y_p + 28Y_{28\mathrm{Si}} + 32Y_{32\mathrm{S}} + 40Y_{40\mathrm{Ca}} + 54Y_{54\mathrm{Fe}} + 58Y_{58\mathrm{Ni}} = 1$$

$$Y_p + 14Y_{28\mathrm{Si}} + 16Y_{32\mathrm{S}} + 20Y_{40\mathrm{Ca}} + 26Y_{54\mathrm{Fe}} + 28Y_{58\mathrm{Ni}} = Y_e$$

$$Y_{\mathrm{SiG}} = Y_{28\mathrm{Si}} + Y_{32\mathrm{S}} + Y_{40\mathrm{Ca}} \qquad Y_{\mathrm{FeG}} = Y_{54\mathrm{Fe}} + Y_{58\mathrm{Ni}}$$

Then, from the defining QNSE relations:

$$\frac{Y_{A,Z}}{Y_{A',Z'}} = f(\rho, T) Y_p^{Z-Z'} Y_n^{A-A'-(Z-Z')}$$

$$f(\rho, T) = \frac{G_{A,Z}}{G_{A',Z'}} \left(\frac{\rho N_A}{\theta} \right)^{A-A'} \exp\left(\frac{B - B'}{kT} \right)$$

$$\theta = \left(\frac{m_{\mathrm{u}} kT}{2\pi\hbar^2} \right)^{\frac{3}{2}}$$

We derive our first result

$$\Phi(T) = \frac{Y_{28\mathrm{Si}}}{Y_{32\mathrm{S}}} \left(\frac{Y_{40\mathrm{Ca}}}{Y_{32\mathrm{S}}} \right)^{1/2} = \exp\left(\frac{-1.25}{T_9} \right)$$

Typical temperatures in QNSE regions where the SiG elements are formed are 3-4×10^9 K; over this range Φ varies from 0.66 to 0.73.

Measuring Φ at a single epoch from the abundance ratios allows a test of whether the SiG material was produced in a QNSE state.

Measuring Φ at multiple epochs when silicon features dominate the spectrum allows trends in the QNSE temperature to be assessed.

Measurement of four quantities Y_{28Si}, Y_{32S}/Y_{28Si}, Y_{40Ca}/Y_{32S}, Y_{54Fe}/Y_{28Si} is a sufficient basis to solve for all the abundances in the silicon-rich region of SNIa.

With a little algebra we derive our baseline recipe:

$$Y_e = Y_{28\mathrm{Si}} \left[14 + 16 \frac{Y_{32\mathrm{S}}}{Y_{28\mathrm{Si}}} + 20 \frac{Y_{40\mathrm{Ca}}}{Y_{32\mathrm{S}}} \frac{Y_{32\mathrm{S}}}{Y_{28\mathrm{Si}}} + 26 \frac{Y_{54\mathrm{Fe}}}{Y_{28\mathrm{Si}}} + 28\Psi \frac{Y_{32\mathrm{S}}}{Y_{28\mathrm{Si}}} \frac{Y_{54\mathrm{Fe}}}{Y_{28\mathrm{Si}}} \right]$$

The first step to reconstructing Y_e is determining the Y_{28Si}/Y_{32S} and Y_{40Ca}/Y_{32S} ratios from observations of strata with similar velocities.

Another step is determining the Y_{54Fe}/Y_{28Si} ratio. Usually ^{54}Fe is difficult to extract from the iron lines. However, ^{54}Fe is the only abundant iron isotope in the regime where both ^{28}Si and ^{32}S are also abundant, in the absence of significant mixing of core material.

Accurate determination of $Y_{^{28}Si}$, $Y_{^{32}S}/Y_{^{28}Si}$, $Y_{^{40}Ca}/Y_{^{32}S}$, and $Y_{^{54}Fe}/Y_{^{28}Si}$ is sufficient to determine Y_e to ~6% because these abundances account for ~94% the QNSE composition.

What are the observational implications of the different combustion mechanisms for the different models?

Craig: The mass density of single degenerate (few$\times 10^9$ g cm^{-3}) and double degenerate (much less) may lead to a discriminant.

Andy: Incomplete burning → extensive carbon.

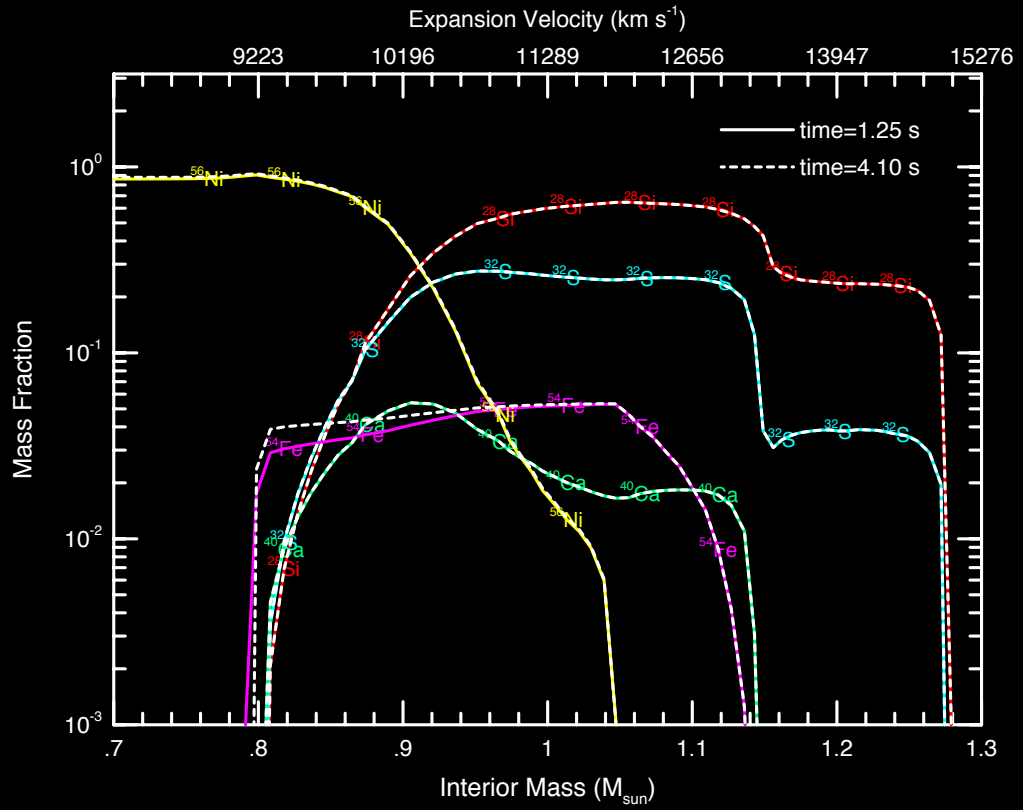

Mass fractions of the major elements during a W7-like explosion. Abundances produced by QNSE conditions at t = 1.25 s are the same as the freezeout abundances at t = 4.0 s.

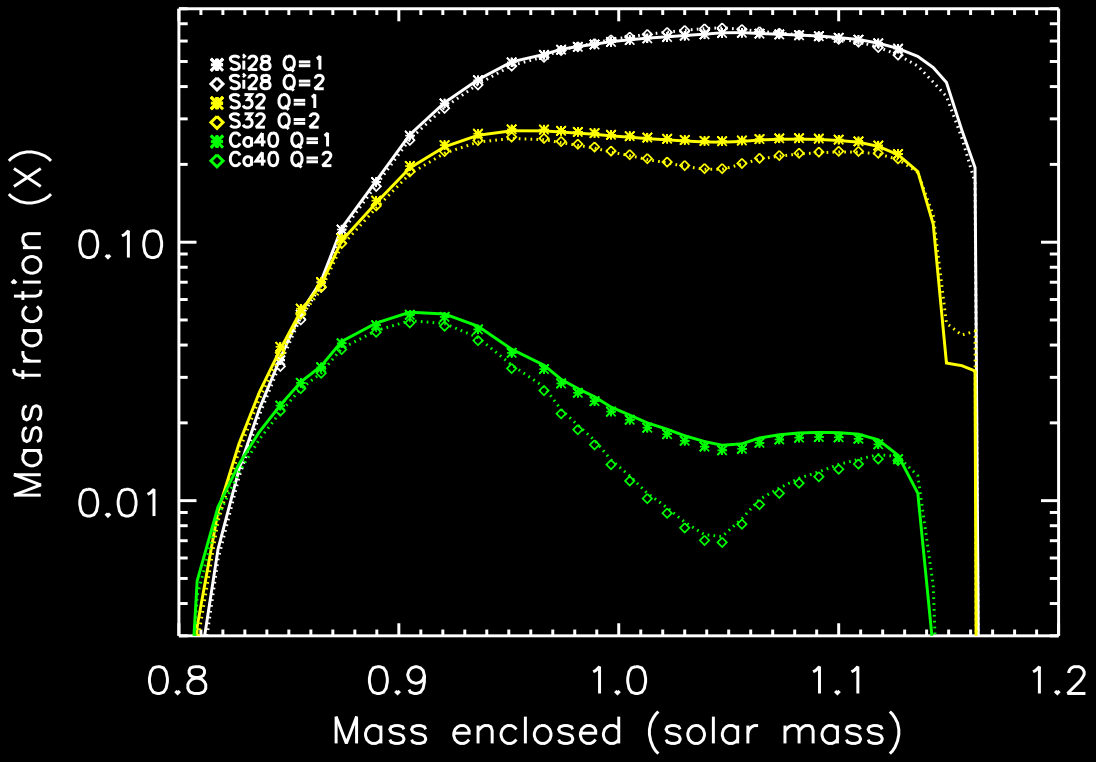

Mass fractions of the major SiG elements versus interior mass for the W7-like models (lines) and QNSE calculations (symbols) at t = 1.19 s. Solar ^{22}Ne(Q=1) and twice solar ^{22}Ne (Q=2) are shown.

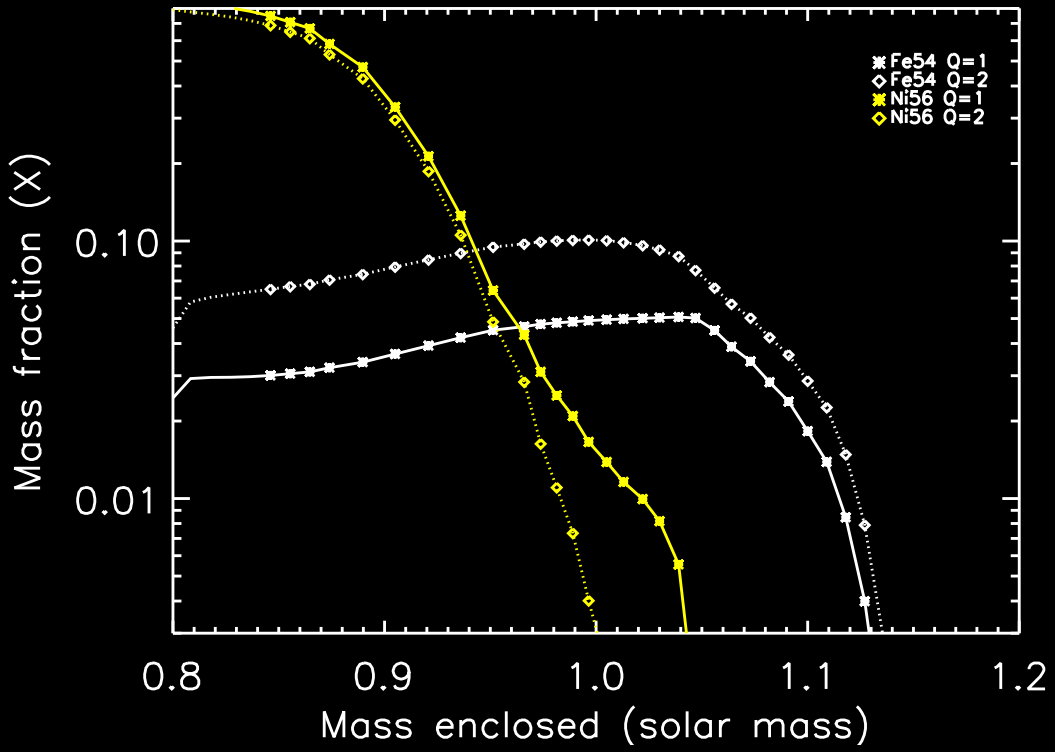

Same, but for the major FeG elements.
^{54}Fe shows the largest change with changes in ^{22}Ne.

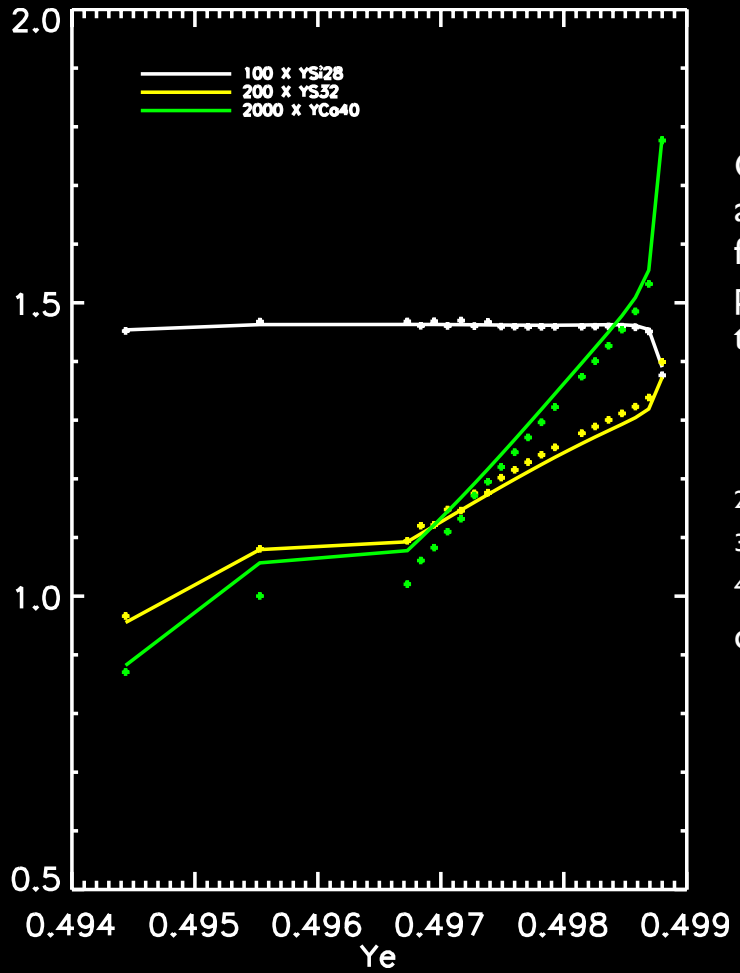

Global abundances of ^{28}Si, ^{32}S, and ^{40}Ca as a function of the electron fraction Y_e produced by the post-processed W7-like models (lines) and the analytical QNSE results (symbols).

^{28}Si is independent of Y_e,
^{32}S shows a near linear trend,
^{40}Ca shows a more complex, but near quadratic, dependence on Y_e.

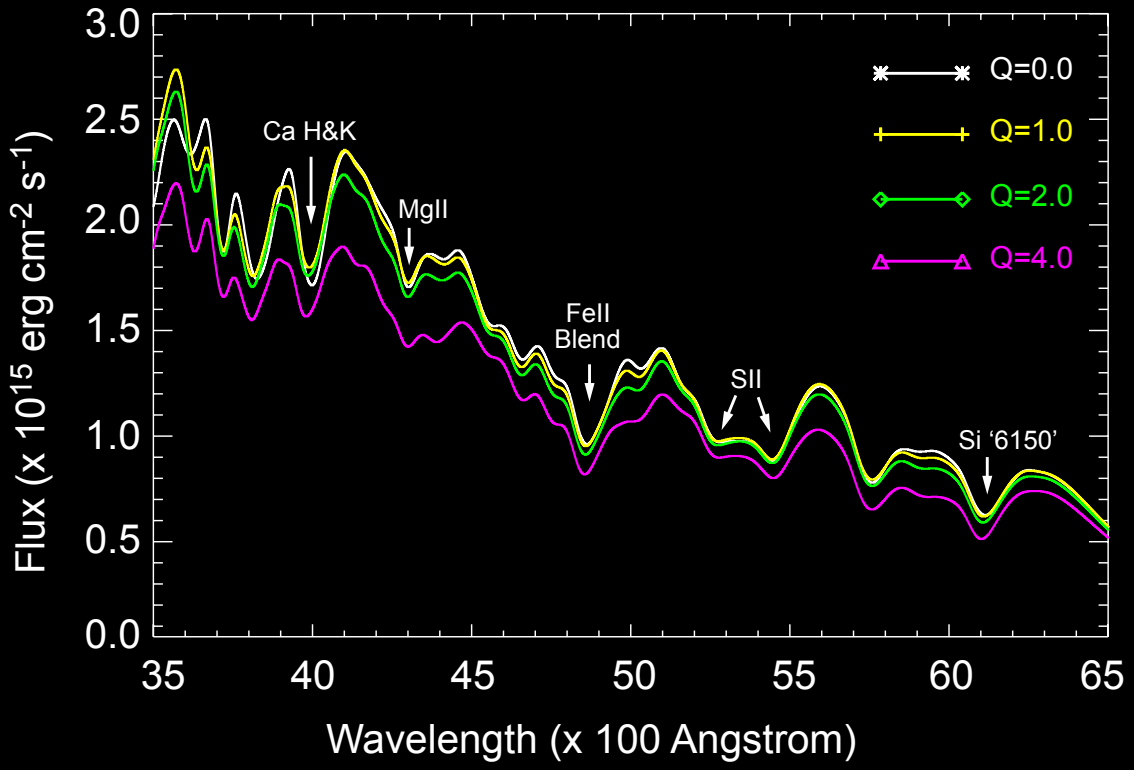

Synthetic spectra for the W7-like models with 0 to 4 times solar 22Ne.

SPIDER

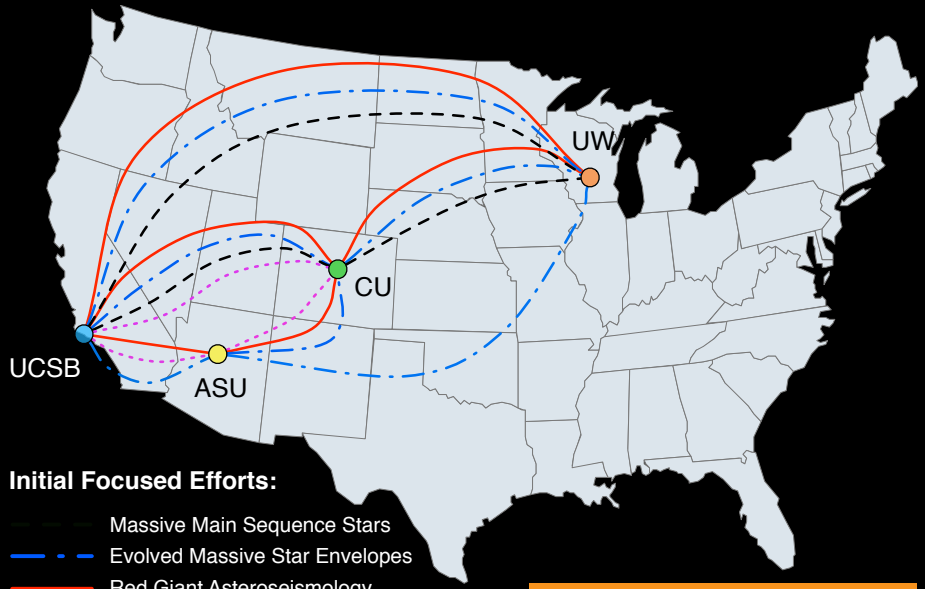

Initial Focused Efforts:

- Massive Main Sequence Stars
- Evolved Massive Star Envelopes
- Red Giant Asteroseismology
- Carbon Burning Flames

The SPIDER Network

Node	**ASU** Arizona State University	**UW** University of Wisconsin	**CU** University of Colorado	**UCSB** University of California Santa Barbara
Fundamental Theory	Stellar Evolution, Flames, Supernovae, Nucleosynthesis	Massive Stars, Asteroseismology, Waves, MHD	Convection, Dynamos MHD, Waves, Helioseismology,	Stellar Evolution, Supernovae, Asteroseismology
Computational Tools	MESA	GYRE	ASH CSS	MESA